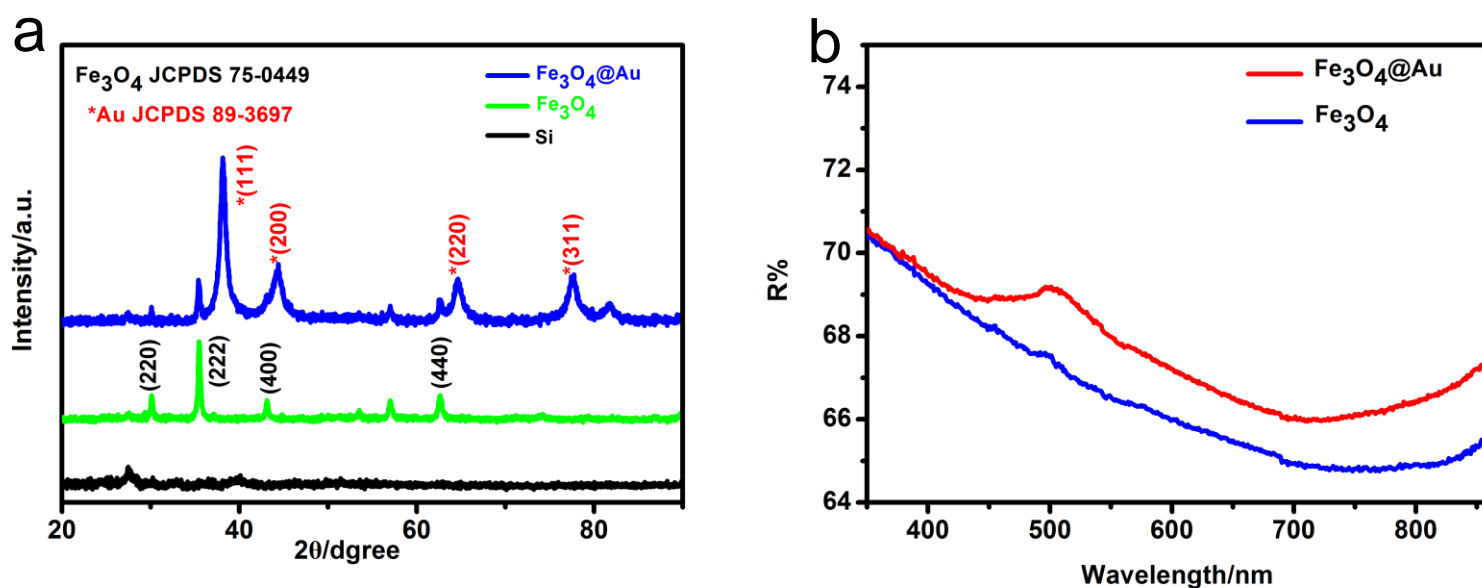
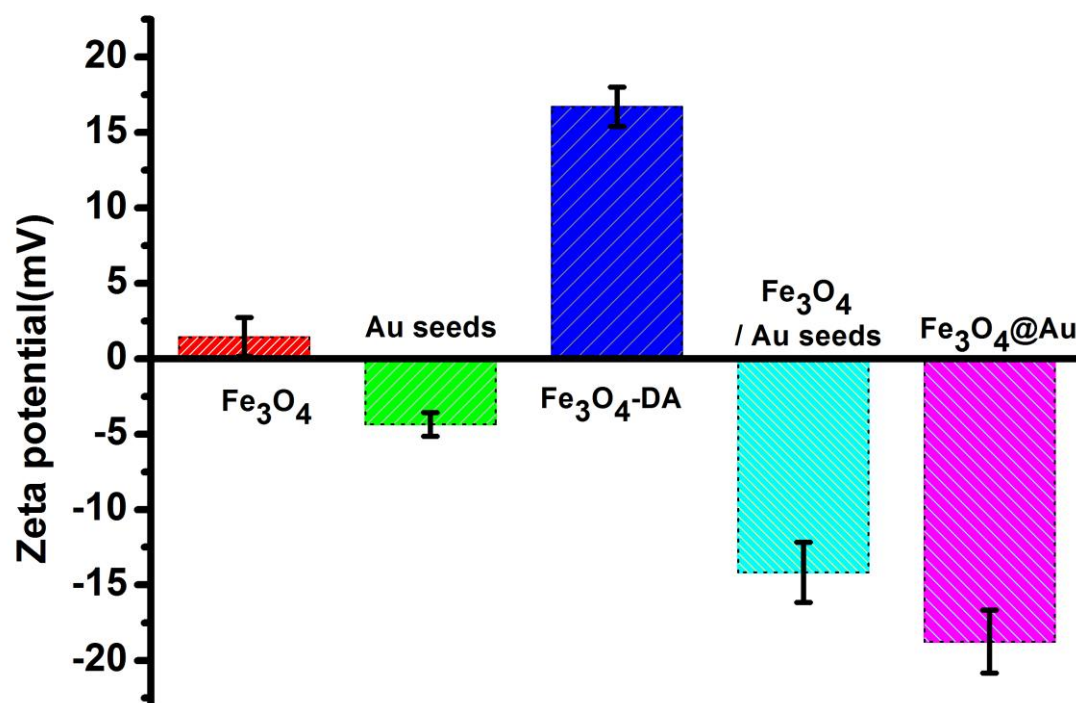


## **Electronic Supplementary information**



**Figure S1.** a) XRD patterns of prepared Fe<sub>3</sub>O<sub>4</sub> NPs (green curve), Fe<sub>3</sub>O<sub>4</sub>@Au NCs (blue curve) and the silicon substrate (black curve, control substrate for XRD) . b) Reflection spectra of the Fe<sub>3</sub>O<sub>4</sub> NPs and Fe<sub>3</sub>O<sub>4</sub>@Au NCs in aqueous solutions.



**Figure S2.** Measurements of Zeta potential of intermediate and final products during the synthesis, error bar : standard deviation (n=3).

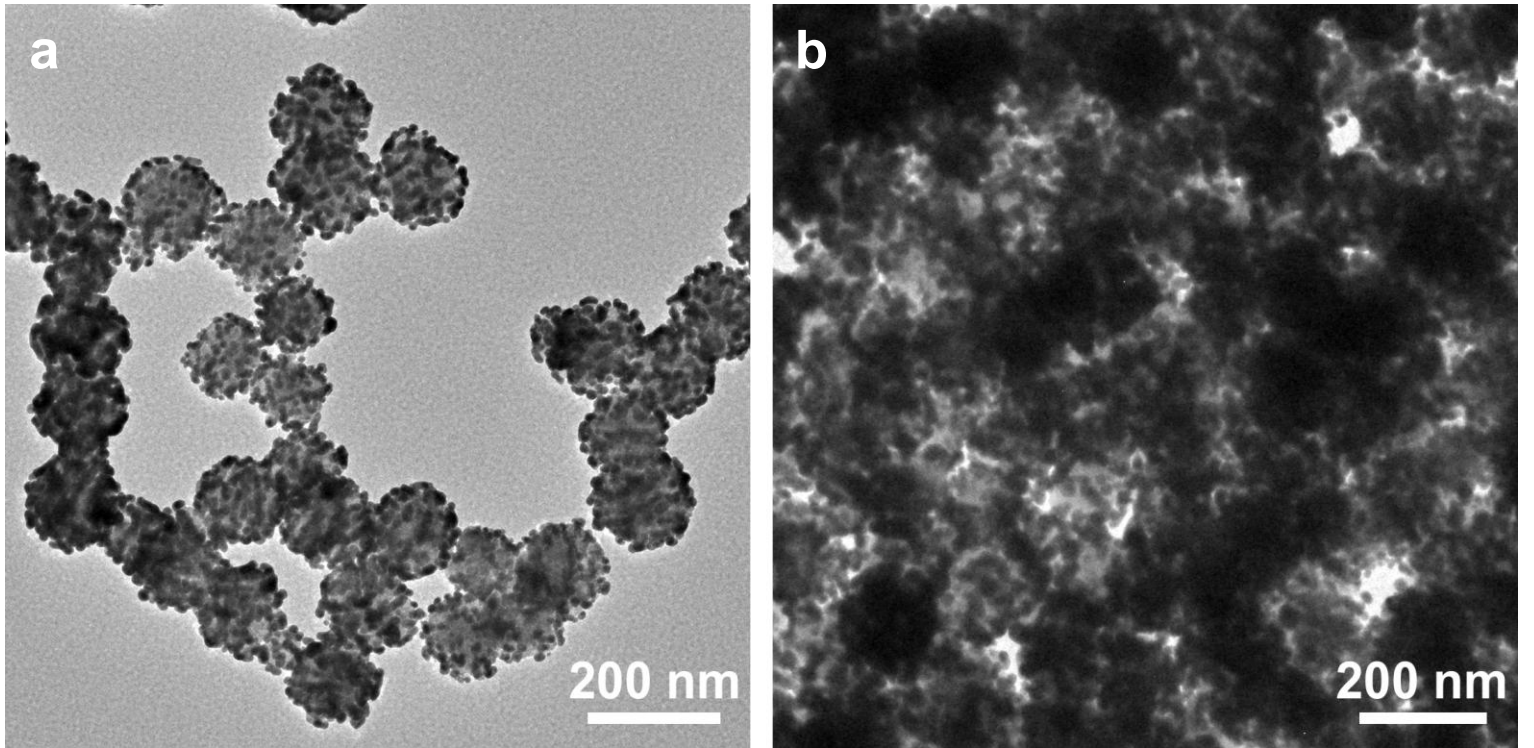


**Figure S3.** TEM images of  $\text{Fe}_3\text{O}_4@Au$  NCs without a) or with b) the external magnetic field.

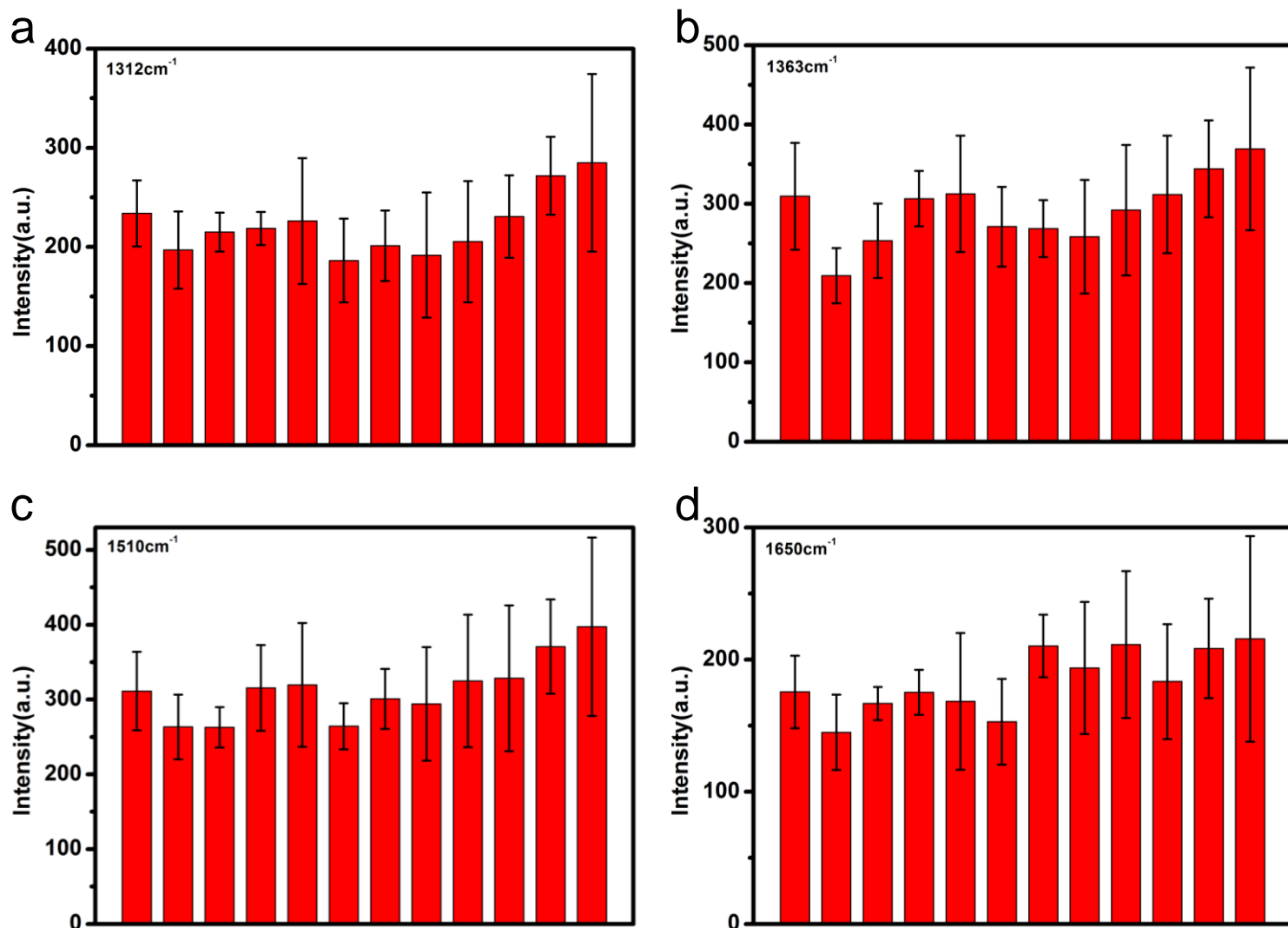


**Figure S4.** Reproducibility of the SERS signals using the silicon-based substrates from different batches, including 12 separate substrate samples, error bar: standard deviation showing well-to-well variations ( $n=5$ ), R6G ( $1 \times 10^{-6}\text{M}$ ).

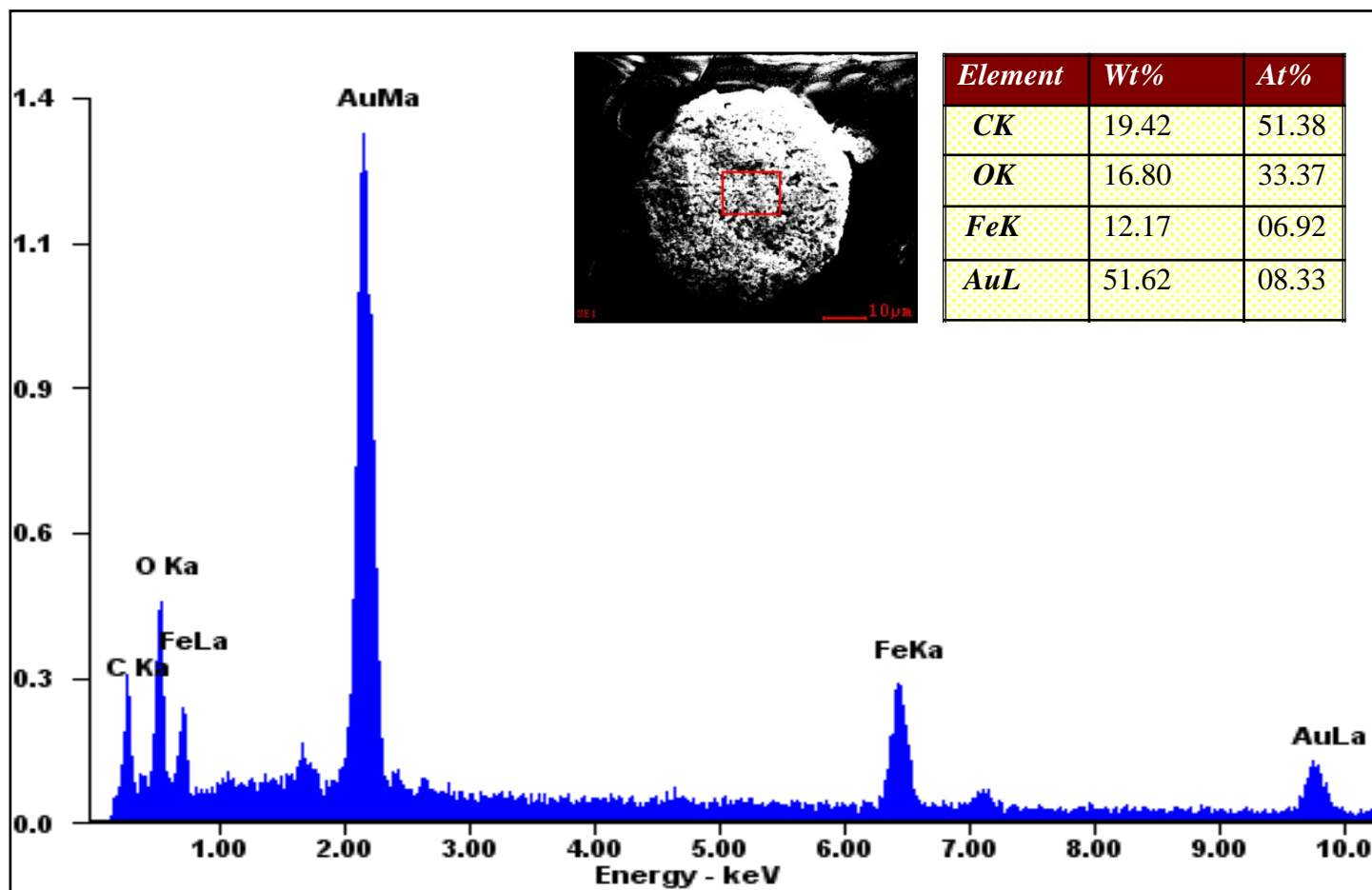


**Figure S5.** The EDS analysis of Fe<sub>3</sub>O<sub>4</sub>@Au NCs on the PAM hydrogel-based substrates, with the insets showing the transfer and the aggregation morphology of Fe<sub>3</sub>O<sub>4</sub>@Au NCs on a single PAM hydrogel micropillar (left), the composition and ratios of the main elements of the PAM hydrogel-based substrates (right).

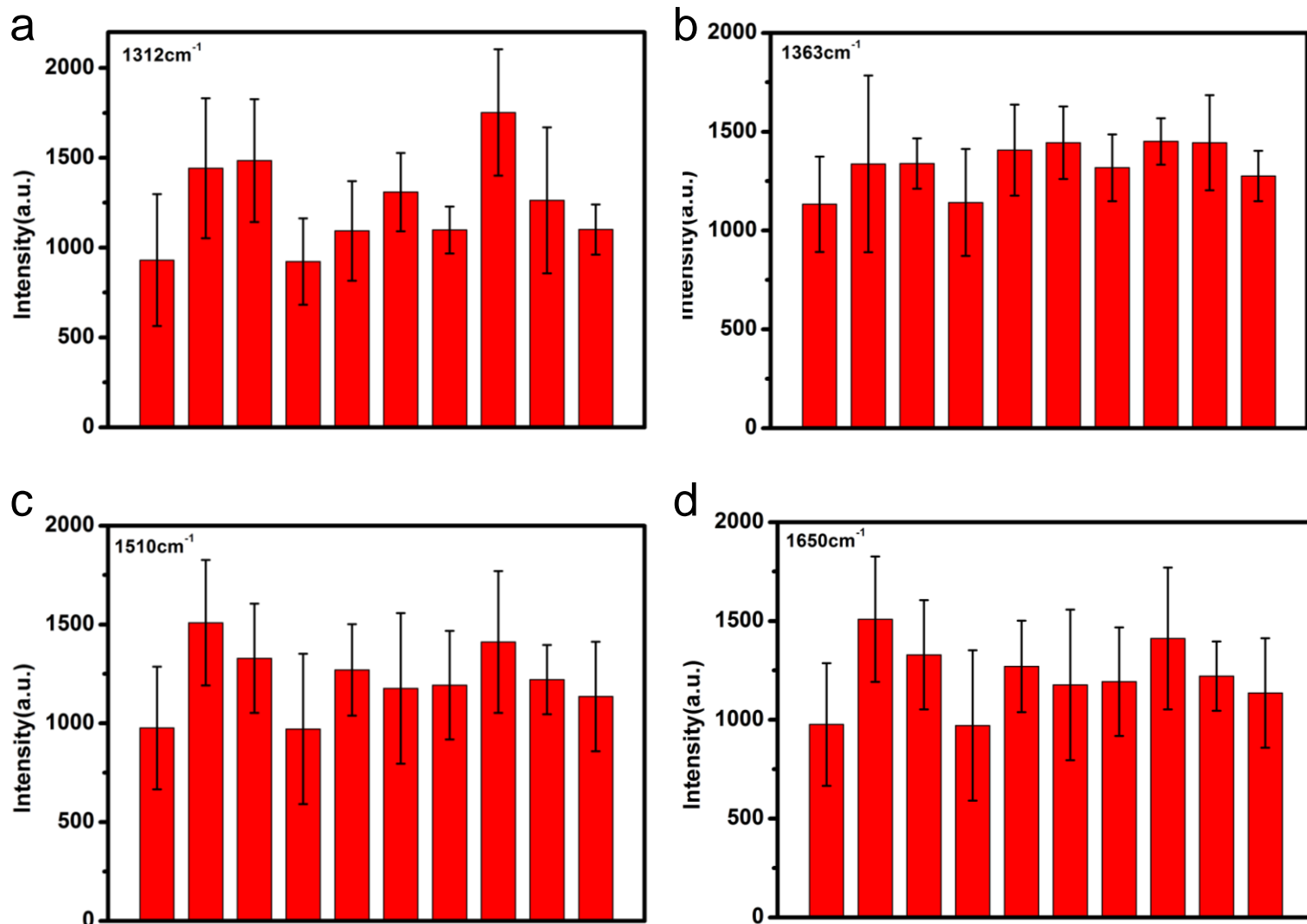


**Figure S6.** Reproducibility of the SERS signals using the PAM hydrogel-based substrates from different batches, including 10 separate substrate samples, error bar: standard deviation showing well-to-well variations ( $n=5$ ), R6G ( $1 \times 10^{-5}$  M).

**Table 1.** Enhancement factors (EF) of different substrates for R6G.

	1312 cm <sup>-1</sup>	1363 cm <sup>-1</sup>	1510 cm <sup>-1</sup>	1650 cm <sup>-1</sup>
Silicon-based substrate	$7.45 \times 10^6$	$7.12 \times 10^6$	$4.95 \times 10^6$	$3.46 \times 10^6$
Hydrogel-based substrate	$1.87 \times 10^6$	$1.03 \times 10^6$	$1.03 \times 10^6$	$0.59 \times 10^6$
Control <sup>1</sup>	$1.59 \times 10^4$	$1.63 \times 10^4$	$1.28 \times 10^4$	$1.03 \times 10^4$
Control <sup>2</sup>	$2.52 \times 10^4$	$3.25 \times 10^4$	$2.61 \times 10^4$	$1.77 \times 10^4$
Control <sup>3</sup>	$1.66 \times 10^4$	$2.54 \times 10^4$	$2.38 \times 10^4$	$1.43 \times 10^4$
Control <sup>4</sup>	$1.57 \times 10^5$	$1.52 \times 10^5$	$1.42 \times 10^5$	$1.32 \times 10^5$

**Table 2.** Relative standard deviation (RSD) of different substrates for R6G.

	1312 cm <sup>-1</sup>	1363 cm <sup>-1</sup>	1510 cm <sup>-1</sup>	1650 cm <sup>-1</sup>
Silicon-based substrate	13.7%	14.7%	13.2%	13.0%
Hydrogel-based substrate	16.6%	14.8%	16.8%	19.2%
Control <sup>1</sup>	82.3%	74.9%	79.3%	87.3%
Control <sup>2</sup>	51.4%	46.5%	34.9%	43.4%
Control <sup>3</sup>	59.7%	61.9%	64.2%	61.2%
Control <sup>4</sup>	68.9%	68.2%	67.7%	66.9%

Note:

control<sup>1</sup>: Fe<sub>3</sub>O<sub>4</sub>@Au NCs deposited into the micro-wells without a magnet.

control<sup>2</sup>: Fe<sub>3</sub>O<sub>4</sub>@Au NCs deposited on the smooth wafer with a magnet.

control<sup>3</sup>: Fe<sub>3</sub>O<sub>4</sub>@Au NCs deposited on the smooth wafer without a magnet.

control<sup>4</sup>: A monolayer of Fe<sub>3</sub>O<sub>4</sub>@Au NCs deposited on the smooth wafer without a magnet. (Reference: Y.J. Li, W.J. Huang, S.G. Sun, *Angew. Chem. Int. Ed.*, 2006, 45, 2537-2539.)

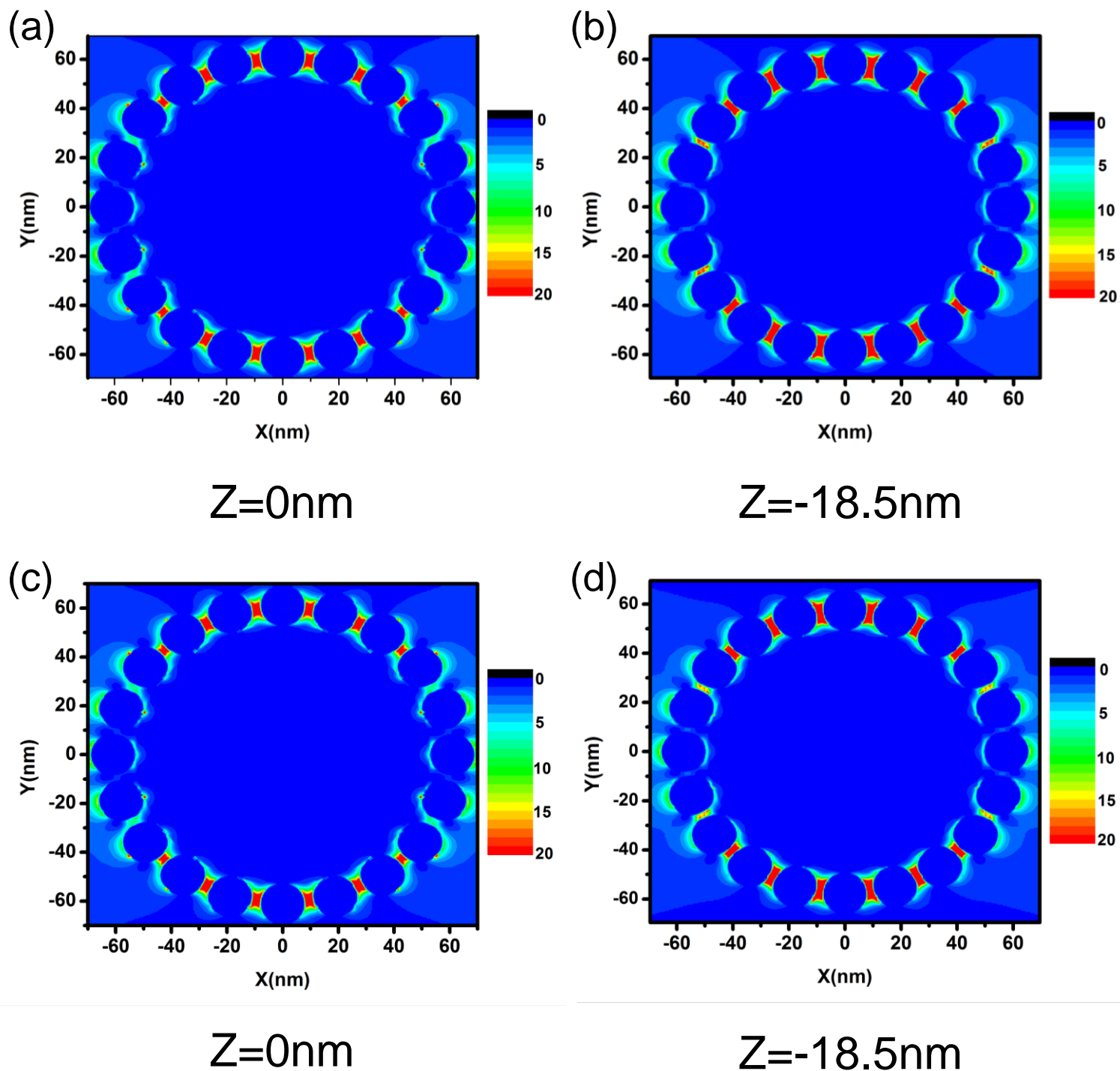


**Figure S7.** Simulated electromagnetic field distribution of the  $\text{Fe}_3\text{O}_4@Au$  NC at the x-y plane of  $z=0$  nm and  $z=-18.5$  nm in the aggregated status, respectively. a-b) Gap distance between NCs: 1 nm. c-d) Gap distance between NCs: 2 nm.